INTERNATIONAL JOURNAL of RENEWABLE ENERGY RESEARCH
M. K. Hammad et al., Vol.13, No.1, March, 2023

Power Quality Enhancement of Hybrid PV-Wind System Using D-STATCOM

Mohamed K. Hammad*, Mohammed Elsayed Lotfy**, Mohamed A. El-Hameed***

*Electrical Power and Machines Department, Sinai University, El-Arish, Egypt

**Electrical Power and Machines Department, Zagazig University, Zagazig, Egypt

**, ***ECEN Department, Faculty of Engineering, A'Sharqiyah University, Ibra 400, Oman.

(Mohamed.khalil4321@gmail.com, Mohamedabozed@zu.edu.eg, M_a_elhameed@zu.edu.eg)

‡ Corresponding Author; Mohamed K. Hammad, Faculty of Engineering, Sinai University 45518 North Sinai, Egypt, Tel: +201004527575, Mohamed.khalil4321@gmail.com

Received: 15.11.2022 Accepted:26.12.2022

Abstract- Power quality (PQ) concerns are considered the most prevalent issues related to the integration of renwable energy sources with electrical power networks. This paper tackles the enhancement of PQ issue regarding hybrid PV-wind system by using D-STATCOM. To do so, optimal parameters of D-STATCOM controller is determined by particle swarm optimization (PSO) and political optimization (PO). To examine the presented system with D-STATCOM based on PSO and PO, a comparison with static var compensator (SVC) is conducted under different operating conditions including voltage malfunction; sag, swell and harmonics distortion. The robustness and feasibility of the proposed technique for improving these issues are tested by using extensive simulation results. The proposed system along with D-STATCOM and its controller are simulated using MATLAB/SIMULINK. During the occurrence of voltage swell, the proposed D-STATCOM system can keep the voltage at appropriate levels, as well as raise the voltage to acceptable levels during the occurrence of voltage sag, in addition to the achieved reduction in total harmonic distortion.

Keywords- Hybrid PV-wind system; Harmonic distortion; Power quality; DSTATCOM; Particle swarm optimization; Political optimization.

1. Introduction

An increasing number of customers utilizing commercial, industrial, traction, and domestic appliances/devices have recently complained about several technical problems associated with power quality (PQ) [1]. In spite of the fact that electronic devices are nowadays involved in modern industrial processes, they are susceptible to malfunctioning. Since these disturbances are the most common ones related to power quality, industrial use finds them challenging to tolerate. Thus, due to the frequent malfunctioning of the system, there is a growing tendency to lessen the effects of such disturbances to the end users. Using various custom power devices is key to overcoming the issues related to PQ. It is worth mentioning that being a concept dependent on power electronics-based devices, Custom power aims to enhance, using distribution networks, power reliability, and quality. One of the main functions of such devices is to mitigate the effects of PQ disturbances in connection with grid codes. Another function is that by using power electronic controlled devices, particularly in a network specified for transmission and distribution, custom power functions as stabilizing the power system. This can be done through controlling power flow and voltage through flexible-a.c-transmission system (FACTS) devices. There are two main categories of FACTS, the first category is based on thyristor-controlled reactors via turn-off thyristor (GTO) which includes static VAr compensator (SVC), thyristor-controlled series capacitor, thyristor-controlled phase angle regulator, etc. The second category is composed of static synchronous compensator (STATCOM), static synchronous series compensator, unified power flow controller, etc. The problems associated with PQ are mainly voltage problems such as sag and swell, harmonics, interruption, fluctuation, unbalance, etc. Such problems have recently become the central focus of interest for several researchers. The consequences of such problems include the following: (1) increase in power losses, (2) slower response time, (3) decrease in the limits of power flow, (4) overheating in electrical machines and neutral, and (5) malfunction of control circuits and computer-based equipment. In addition, the power uniformity of demand is influenced by PQ in that the amount of the tariff is particularly affected. Accordingly, enhancing PQ is an essential issue that benefits the customer. In an attempt to bring about balancing within the distribution system on both sides: the load and source sides. Towards this end, using power electronic devices such as D-STATCOM (shortened for the distribution static compensator) is an effective method. When it comes to compare D-STATCOM with other compensation devices, it is found that it is featured with several advantages, which include the following: (1) power losses tend to be low, (2) generating a few harmonic elements, (3) the ability to withstand high regulation, low cost, and small size, (4) facilitating compensation because it does so in fast and inductive mode quickly and without interruption, and (5) can be connected to point-common-coupling (PCC) in the distribution system that contains non-linear loads. Additionally, when you set a particular load where the total amount required meets the facility delivery specifications, D-STATCOM can pump enough of the late or early compensation stream. D-STATCOM is likely to serve a key function in radiological distribution systems due to increased load demand. D-STATCOM performance depends on the control algorithm.

Proportional-integral controllers (PI) along with its fixed parameters serve as observing and achieving D-STATCOM control. Several related studies have investigated D-STATCOM controllers. In [2], focus on enhancing voltage sag by using SVC and DSTATCOM. This voltage sag is the result of sudden heavy load and short circuits faults. Authors in [3], highlights three various control techniques to obtain the reference current components for DSTATCOM device. In order to optimize and regulate the voltage, the authors in [4] proposed a special design of the nonlinear controller for DSTATCOM, which is connected to the power distribution system with distributed generation (DG). Furthermore, for different harmonic compensations and power factor correction, researchers in [5] introduce a powerful adaptive control technology for the active power filter. The authors in [6] analyzed, to improve the PQ of a power distribution system, a sliding mode controller based on DSTATCOM. In addition, researchers of [7], in order to compensate for multiple loads in the electrical distribution system, shed light on the performance analysis of the FPGA-controlled quadrupole DSTATCOM. A three-phase synchronous static compensator with five branches to be connected to a multi-ground distribution network is introduced in [8]. In [9], the researchers tackle the optimal allocation and sizing of DSATACOM through the use of the Harmony Search algorithm to lessen the network total power losses. Furthermore, researchers in [10] point to the allocation of DSTATCOM in the energy distribution system taking into account pregnancy fluctuations using the bat algorithm to reduce energy loss. In [11], the authors mentioned the simultaneous multi-goal customization of DG and DSTATCOM in radiological distribution networks through the cuckoo search algorithm. The authors in [12] addressed voltage control by proposing a new technology to improve D-STATCOM performance in the power grid to reduce current harmonics and voltage and improve the power factor in the electrical system. Researchers in [13] compare various control techniques and control approaches such as instantaneous interactive power theory, simultaneous frame reference frame theory, instantaneous symmetric component theory, and enhanced second-degree generalized integrator squaring signal generator are used with D-STATCOM to work on PQ issues. The authors in [14] refer to the effect of DSTATCOM in which PV is largely penetrated in a micro-grid, that is connected to the distribution system, this in turn, has an impact on the poor utility distribution system, resulting in difficulties including voltage dip(sag), swell, imbalance, harmonics, and DC current injection. In [15], the authors used a self-adjusting filter based on instant interactive energy theory to improve the D-STATCOM control algorithm. The authors in [16] provide a special control technique for DSTATCOM by the fuzzy-PI current controller. The authors in [17], provide a control technique for DSTATCOM based on consumer-generated voltage imbalance estimation. Using measurements of instantaneous currents and PCC voltages, the suggested method must qualify the parcels of imbalanced voltage due to the consumer utility. The researchers in [18] discuss the PQ enhancement based on five level shunt APS using sliding mode control scheme connected to a PV.

The D-STATCOM concept is mainly based on the FACTS conversion device. This device acts as a linear effort regulator for PCC, balancing loads or compensating for the interactive power of the load by generating the size and stage required for the inverter output voltage, which is connected to a continuous current capacitor (i.e. a power storage device). Voltage source-inverter (VSI) are available as well as many diverse D-STATCOM configurations. Various strategies are also available including the integrated relative control, slide mode controller, and non-linear control unit for DSTATCOM control.

Due to D-STATCOM nonlinear operation, the nonlinear controller will be favored over the linear method. Voltage dynamics can be improved by reducing and regulating the capacitor DC voltage in D-STATCOM. Non-linear control depends mainly on fine sin through feedback. A PI controller is available in this control system to repair the voltage. Additionally, a few selected sets of PI parameters may not be suitable for all operating point ranges, so these values are complex and time-consuming. In order to control adapter streams that lead to rapid control of the interactive current, vector control techniques can be used to perform this function.

In the process, in order to find optimal values for the PI gains, the powerful and well-known optimization algorithms called PSO and PO are applied. The use of PSO and PO, which are a computational methods help iteratively optimize a problem in an attempt to find a solution with reference to a given measure of quality. In order to show the improvement that occurred to convergence speed, error reduction, voltage disturbance, and other circuit parameters, the new added PI coefficients, calculated in these ways, are carried out in controller with different study cases such as voltage sag, swell, and harmonic evaluation.

2. Parameters of Power Quality and Their Consequences

2.1. Harmonics-Distortions

Considered one of PQ problems. viewed as current or voltage sine-wave's periodic deviation from a smooth sinusoidal shape, it occurs when the multiple integers frequencies of the F_0 (shortened for fundamental frequency) are supplied to the proper functional current's or voltage's sinusoidal waveform. Therefore, harmonics can regard as multiples of F_0. THD (shortened for total harmonic distortion) is referred to as a measure of all the distorted values of the waveform.

Harmonics-related malfunctions can be attributed to non-linear loads. This includes electronic devices and equipment in which voltage or current in a normal sinusoidal shape is not used. Examples of these cover computers, electronic ballasts, television, arc furnaces, arc welders, mercury lamps, battery chargers, drives with variable speed, equipment used for medical diagnosis, and fluorescent lamps at the receiving (consumer) end. Origins of harmonics include resonance phenomena, switch mode related to power supply transformer saturation, light dimmers, and, which are considered a few of the numerous instances available. A huge damage to transmission, distribution system and consumer equipment can occur by means of harmonic distortions. The most prominent effects caused by harmonics-related distortion include nuisance tripping of circuit breaker, overload operation of electric motor, fuses malfunctioning, overheating of transformers electric motors and, tripping of variable speed drives, power measured incorrectly resulting in failure or damaged electrical equipment such as power factor that needs correction as well as capacitors and contactors.

The use of passive filters, application of active conditioner, and isolation transformers can help mitigate harmonic distortions. The electrical devices with built-in power factor correction are also used to reduce harmonic distortion. Furthermore, FACTS devices such as SVC, DVR, and D-STATCOM are used to mitigate the THD given by Eq. (1) in the electrical power system.

$$THD_v = \frac{1}{V_1} \times \sqrt{\sum_{h=2}^{N} V_h^2}, \quad THD_I = \frac{1}{I_1} \times \sqrt{\sum_{h=2}^{N} I_h^2} \qquad (1)$$

The THD value in rms of the waveform when the basic waveform is deleted, as shown in equation (1). The system frequency (50 or 60 HZ) is represented in the fundamental smooth sinusoidal voltage. Where V_1 represents the fundamental voltage, I_1 the fundamental current, and V_h the harmonic voltage [19].

For 11 kV, the voltage THD should be less than 5% as given in IEEE519-2014 and shown in Table 1.

Table 1. Voltage distortion limits according to IEEE519-2014.

The voltage at PCC	Individual Harmonic (%)	Total harmonic distortion THD (%)
V ≤ 1.0 KV	5.0	8.0
1 KV < V ≤ 69 KV	3.0	5.0
69 KV < V ≤ 161 KV	1.5	2.5
161 KV < V	1.0	1.5

2.2 Voltage Sag

Voltage sag is one of PQ problems, it is mostly related to power system faults, sudden heavy load, energizing transformer, switching of power lines, large induction motors starting, and the lightning stroke. Voltage sag can be defined as the decreasing of the voltage magnitude from 0.1 to 0.9 per unit for the duration between 0.5 cycle to one minute.

Voltage sag at the point of interconnection (POI) or PCC ΔU_d can be described as a function of rated total power S_n, grid total power short circuit S_k, voltage variation factor $K_u(\varphi_k)$, and phase change φ as given by Eq. (2) [20].

$$\Delta U_d = 100\, K_u(\varphi_k) \frac{S_n}{S_k} \qquad (2)$$

The voltage sag occurring has a bad effect on the power system performance. It can cause the loss of all the data, shut down, and sensitive loads disconnection. Light flicker, transformer failure, variable speed drives tripping, motors overload operation, and loss of controller memory or computers are viewed as other effects of voltage sag. A fault in the transmission line can damage sensitive loads up to hundreds of kilometers away from the fault.

The addition of devices like a ferro resonant transformer, sag proofing transformer, UPS, coil-hold in devices, flywheel and MG (motor-generator), STATCOM, SVC, and DVR (dynamic voltage restorer), also known as FACTS devices, can reduce voltage sag depending on the state and location of the power system.

2.3 Voltage Swell

Considered one of PQ issues, the swell associated with voltage is viewed as the increase in the voltage magnitude from 1.1 to 1.8 per unit for the duration between 0.5 cycle to one minute. At the POI or PCC, voltage swell (ΔU_s) can function as the turbine's maximum total power, S_{max}, grid total impedance (resistance, *R*, and reactance *X*), U_n describe the grid's nominal voltage, and the angle of phase shift, φ as described by Eq. (3) [21].

$$\Delta U_s = \frac{S_{max}(R\cos\varphi - X\sin\varphi)}{U_n^{\,2}} \qquad (3)$$

Occurring in electrical power system, the voltage swell can cause a lot of problems such as insulation breakdown, disconnection of electrical devices, equipment mal-function, failure of the correction capacitor of the power factor, weakness of electric conductor, light flicker, variable speed drivers' tripping. Mostly voltage swell occurs because of switching a capacitor bank or a sudden drop of electric loads, the unsymmetrical faults, opening the neutral connection, and a heavy change like starting up or shutting down of large capacity and power line switching.

Using a transformer with a tap-changing to connect a lot of large loads at the PCC can help the voltage swell to be reduced. Also, FACTS devices such as D-STATCOM can be used to mitigate the voltage swell and provide a smooth connection.

3. Distribution Flexible a.c Transmission System (D-FACTS)

3.1 Static VAr Compensator)

SVC is considered one of the most important FACTS that can inject or absorb reactive energy into the electrical power system. It is consisting of the incorporation of thyristor-switched capacitors (TSC) and thyristor control reactors (TCR). The SVC is used to support the voltage and regulation. Also, SVC is used to temporarily enhance the stability and power system oscillation-damping. SVC has the ability to increase power transfer capacity, reducing the line losses, and compensating the electrical grid with the demand reactive power. Also, SVC can be used to solve a lot of problems related to power quality. Examples include harmonics-related distortion, voltage sag, voltage swell, make-up for voltage oscillations, control transmission voltage, and enhancing and stabilizing the grid [22].

3.2 Distribution static compensator

Given the fact that D-STATCOM is an essential device in an electrical power system, it can solve voltage sag, voltage swell, flicker and fluctuation, distortion of current, and three-phase voltage, which is unbalancing in comparison with other types of devices. Therefore, much attention is paid to D-STATCOM in the field of the distribution system and the development path of the reactive power compensation and PQ control at present time. In addition, the D-STATCOM is characterized as fulfilling a powerful function and excellent performance regarding fast load compensation, small size virtue, quick response, little noise, and to many others. With the rapid development of power systems, D-STATCOM is going to be an important component of modern distribution systems. Thus, it will assimilate the traditional SVC and grow to be an essential device to improve the PQ system.

D-STATCOM is regarded as one of GTO based FACTS family. This connected device consists of three legs voltage source converter (VSC) having inductors and six IGBTs and d.c energy storage. Considered a synchronous condenser, it can also provide variable reactive power and monitor the bus voltage in which D-STATCOM is functional. Moreover, D-STATCOM can make available fast energy response or sustain an even better response when compared with a synchronous condenser. Using a coupling reactor or coupling transformer, the three-phase generated voltages are connected to the electrical power system grid. Better control of the flow of active and reactive power between the distribution network and D-STATCOM is possible thanks to both the phase-correct modification and the magnitude of DSTATCOM's output voltage [23].

The controller of D-STATCOM compares the two voltage signals coming from the grid V_l and D-STATCOM voltage V_{st}. If the two signal are equal no power (active or reactive) transfer between the grid and D-STATOM. If the magnitude of PCC voltage is larger than D-STATCOM voltage, in this case, the device will operate as an inductive reactance and take in the reactive power and the inductive current will flow from the grid to D-STATCOM. In the last condition, if the voltage magnitude of D-STATCOM is larger than PCC voltage, the device will operate as capacitive reactance and the current will flow from the D-STATCOM to the power system.

A schematic of the D-STATCOM control circuit is shown in Fig. 1. Phase-locked loop (PLL) primary function is to synchronize GTO pulses to system voltage and generate a reference angle. As a result, using the transform from a-b-c to d-q-0, the reference angle can be used to determine the positive sequence component of the D-STATCOM current. The voltage regulator block, as shown, can calculate the difference between the measured and reference voltages, and the output is routed through a PI controller to give the reactive current reference (I_{q_ref}). The angle is then created by passing the (I_{q_ref}) through a current regulator block. The current regulator block is made up of a PI controller, whose job it is to keep the angle close to zero. Using the PLL output and the current regulator block, the firing pulse generator block can generate square pulses for the inverter. In the case of a pulsed load, bus voltage can help to reduce the voltage regulator's power consumption. So that more active power can flow from the bus to the D-STATCOM and enable the capacitor to be powered, the current regulator can advance the angle [24].

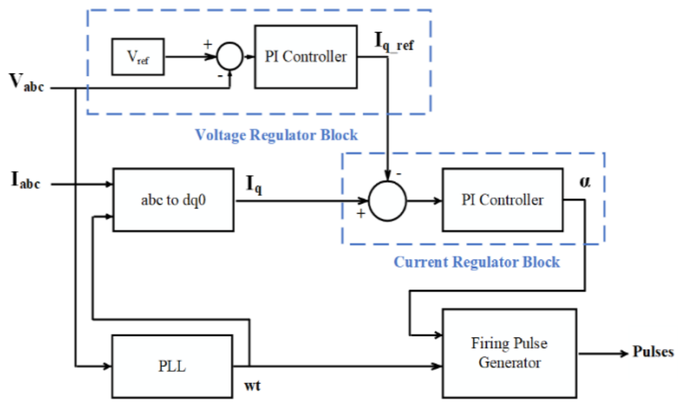

Fig. 1. Control structure for the D-STATCOM.

As a result, the DC voltage rises, the inverter's AC output rises, and necessary reactive power flows from D-STATCOM to the system. Electrical power (active or reactive) exchange between the system and D-STATCOM equations can be described by Eq. (4) and (5).

$$P = \frac{V_{pcc}V_{st}}{X_t} \sin \delta \quad (4)$$

$$Q = \frac{V_{pcc}^2}{X_t} - \frac{V_{pcc}V_{st}}{X_t} \cos \delta \quad (5)$$

where the active power is represented in P; Q is the reactive power; V_{pcc} is the voltage at PCC; V_{st} is the D-STATCOM voltage; X_t is the total line reactance; δ is the angle delta between bus voltages.

4. Heuristic Optimization Algorithms

4.1 Particle swarm optimization

One contemporary algorithm that can be used to solve non-continuous and non-linear optimization problems is the PSO algorithm [25]. PSO method can be used to handle a variety of power system challenges, such as optimal power system stabilizer design, estimation of distribution state, and optimal reactive power dispatch. Being a heuristic search or optimization technique, PSO is inspired by the teamwork behaviors of those birds and animals such as flocks of birds or schools of fish. The birds or fish hereafter, for instance, use a complex means of communication (i.e., hence particles used as a term) to communicate with each other. Aside from the skills of communication that they possess, the particles are featured with continuously modifying and upgrading the best performances from the past ones in the current flight [26].

Each particle in the PSO model for industrial optimization is linked to several parameters. A vector represents the various parameters that have been specified for each particle. All of the particles are represented by an equal number of elements in the vector, which is the same size as the vector to be optimized in the application. To begin, the elements of each particle's vectors are given haphazard values within the permitted range. The performance of each vector is computed using haphazard values for the elements of the vector. The PSO method is a heuristic search approach for finding a specific point in a space that is multi-dimensional, where, as demonstrated, this spot is eventually pointed out by all the particles that meet the goal to be achieved [27]:

$$v_i^k = wv_i^k + c_1r_1(pbest_i^k - x_i^k) + c_2r_2(gbest^k - x_i^k) \quad (6)$$

$$x_i^{k+1} = x_i^k + v_i^{k+1} \quad (7)$$

$$w = w_{min} + e^{(-(20t/t_{max})^2)}(w_{max} + w_{min}) \quad (8)$$

Where V_i^k represents the velocity of the ith particle at iteration kth and X_i^k represents the current solution or position of the ith particle at iteration kth. The path of each particle in the allocated search area is p_{best}, and the prime value secured by a particle at the full swarm is g_{best}. The positive constants are c_1, c_2, and r_1, r_2 are two random variables with a uniform distribution between zero and one. w_{max} and w_{min} are the inertia weight's maximum and minimum values [28]. The PSO algorithm was used to determine the optimal values of D-STATCOM control circuit (K_p and K_i) by connected the SIMULINK file (proposed system) with PSO m-file. The MATLAB running was take a long time to calculate the optimal values which investigate the objective function. The operation time depending on the size of the swarm "number of birds or particles", maximum number "birds steps or iteration" and also depending on laptop specification (RAM, processor and operating system). This work was carried out on a laptop of its specifications (4.00 GB RAM, CORE i5 processor and windows 10). Number of iteration was 100 iteration and number of particles were 11 particles. MATLAB running was take about 48 hours to calculate the optimal values. After determining the optimal values, they are entered into SIMULIK file to examine the proposed system with power quality issues.

4.2 Political Optimizer

The political optimizer (PO) is a socio-inspired meta-heuristic optimization algorithm based on human behavior. It is based on the functioning of political institutions as well as the electoral process. It is modelled after typical steps in establishing a government, such as elections, parliamentary business, constituency elections, members defecting from one party to another, and, in general, election campaigns held by all stakeholders [29]. The dual-sided approach of this algorithm makes it efficient in finding the final global minimum solution. In the first strategy, each candidate for a solution tries to win an election, whereas in the second strategy, each competing political party tries to win a majority of seats in parliament in order to form a government.

The algorithm's exploratory and exploitation phase is the process by which existing solutions are improved. Finding the global minimum solution is aided by this. By changing their position on the solution-search space, which is determined by their prior position, the position of the constituency winner, and the position of the party leader, each candidate can increase their fitness. Additionally, party switching takes place, in which members are transferred from one party to another and the newly arrived member takes the place of the party member with the lowest fitness. After these two procedures are finished, the updated objective function values (fitness) are calculated to determine the new constituency winners and party leaders. Then, during a process known as "parliamentary affairs," random position changes are introduced, and if they increase the fitness value, the new location takes the place of the old one. Repeating the procedure up until the user-defined stopping criteria are satisfied. Political parties' n makes up the population P, as shown in Eq. (9). According to Eq. (10), each party p_i has n candidates or members. As shown in Eq. (11), every jth member p_i^j is a potential solution and is a d-dimensional vector. The value of d represents the quantity of input variables used to formulate the equation, and $P^j_{i,k}$ stands for the kth dimension of P_i^j.

$$p = \{p_1, p_2, p_3, \dots, p_n\} \quad (9)$$

$$p_i = \{p_i^1, p_i^2, p_i^3, \dots, p_i^n\} \quad (10)$$

$$p_i^j = [p_{i,1}^j, p_{i,2}^j, p_{i,3}^j, \dots, p_{i,d}^j]^T \quad (11)$$

A potential solution performs the duties of both a party member and an election candidate. Assumedly, there are n constituencies, as shown in Eq. (12), and the jth candidate from each party runs in the jth constituency, C_j, as expressed in Eq. (13). There is only one parameter n that needs to be tuned for this logical division. The number of parties, constituencies, and candidates in each party are all set to the same value, n, in our mapping.

$$c = \{c_1, c_2, c_3, \dots, c_n\} \qquad (12)$$

$$c_j = \{p_1^j, p_2^j, p_3^j, \dots, p_n^j\} \qquad (13)$$

This algorithm was chosen after analyzing its performance against a number of well-known optimization algorithms for optimal PI controller value (K_p, K_i). During the analysis, the performance of another efficient algorithm known as the PSO was also tested, and it was discovered that the PSO and PO produce similar results.

5. The PI controller tuning techniques

All control systems are primarily responsible for adjusting the error value between the actual value and the reference space at zero. The error is to enter the console in the PI controller, and this input must become zero. The error route is determined from the maximum value to the final minimum value or zero value, depending on the installation properties and the characteristics of the K_p and K_i parameters used in the PI console. The standard PI controller is shown in Figure 2 in the factory's feedback control system.

The constants K_p and K_i employed in PI controllers play a significant role in rectifying faults where performance characteristics such as excess, transient duration, oscillations, and stable status error are minimum for a plant with a given function. If the plant is being studied in writing, the right selection of K_p and K_i parameters for PI controllers can be made using the trial and error method. Specialized tuning procedures are necessary for more complex stations with high transmission function requirements. PSO and PO are a technology that can handle a large number of control equations and constraints and find the best answer. Using PSO and PO technology, a repeating procedure can be used to find K_p and K_i values, as demonstrated in this study. The main purpose of tuning the PI controller is to achieve an acceptable voltage and THD value according to IEEE standards $V_{min} \leq V_{pcc} \leq V_{max}$,$THD \leq 5\%$. When you tweak the PI controller, you get a two-dimensional search space with K_p and K_i values to estimate, (K_p= 2.904, K_i= 1.21).

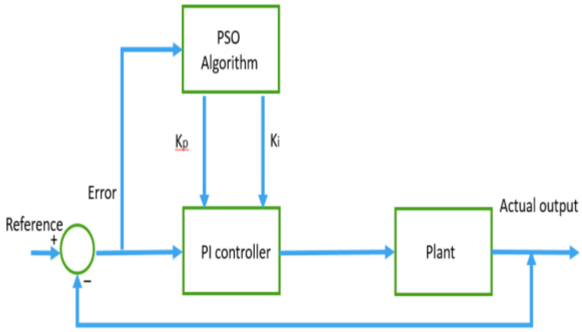

Fig. 2. Typical PI controller

6. System Under Study

The hybrid system is the integration of two or more renewable or conventional power generators. In this study, the proposed hybrid system consists of a photovoltaic group and a wind power plant. The proposed model consists of an electrical power system grid (50 Hz, 11 KV) connected to PV array 0.6 MW, a doubly fed induction generator (DFIG) based wind turbine of 1.2 MW, R-L load, capacitor bank, nonlinear load (universal bridge) connected to the system by the switch to generate harmonic and optimization technique block (PSO) or (PO) to determine the optimal value for D-STATCOM control circuit (K_p, K_i) as indicated in Fig. 3.

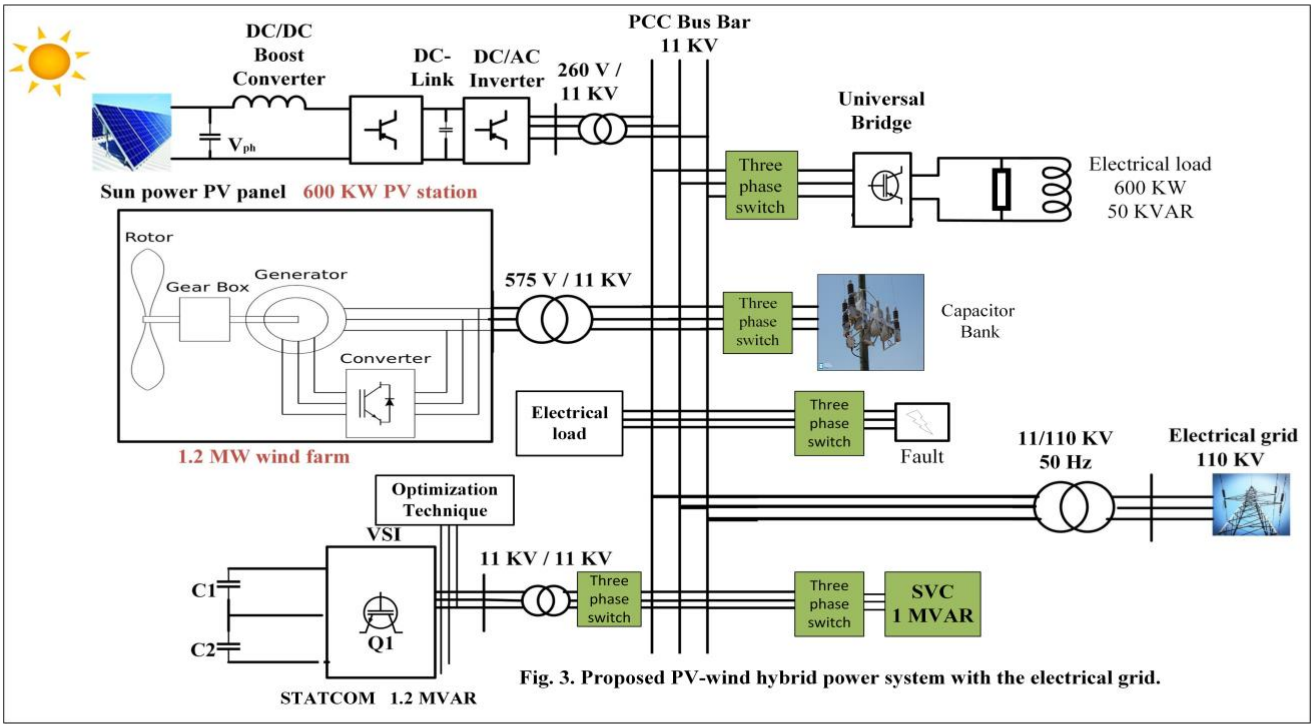

Fig. 3. Proposed PV-wind hybrid power system with the electrical grid.

Wind energy is regarded as one of the primary alternatives for replacing fossil resources in future human society's power consumption. Also considered one of the most important clean sources and it is can supply the electrical network with the demand power without causing any environmental problems.

DFIG is able to convert the mechanical energy to a.c electrical energy, Then the electrical energy transfers to the gird by interconnection lines to supply the electrical loads. The advantages of DFIG are high reactive power support performance, high energy capture capability, less acoustic noise, and lower power rating than back-to-back power converters. Power from variable speed wind turbines based on DFIG is transferred to the grid via two main paths. It is worth noting that the majority of the power is transmitted via the stator, with only a small portion fed through the rotor circuit and converters. The first converter, known as the rotor side transformer, is linked to the rotor coils of the DFIG. The other is known as the network side converter and is connected to the network via an AC filter in the PCC. The electrical energy provided by DFIG to the system can be summarized as follows [30,31]:

$$P_a = \frac{1}{2}\mathcal{P}_{air}\,\pi R^2 C_p(\lambda,\beta)\,V_W^3 \tag{14}$$

$$T_m = \frac{P_a}{w_t} = \frac{1}{2\lambda^3}\mathcal{P}_{air}\,\pi R^5 C_p(\lambda,\beta)\,w_t^2 \tag{15}$$

$$P_{ref} = \frac{\mathcal{P}_{air}\,\pi R^5}{2G^3}\,\frac{C_{p-max}}{\lambda_{opt}^3}\,w_{m-opt}^3 \tag{16}$$

where P_a is the aero-dynamic power extracted by a wind turbine, T_m is the mechanical torque of the wind turbine, P_{air} is the air density, R is the turbine radius, V_w is the wind speed, w_t is the turbine rotational speed and $C_p(\lambda,\beta)$ refers to the aero-dynamic efficiency of the wind turbine.P_{ref} is the active power that the wind power system must supply to the power system depending on the optimal rotational speed $\omega_{m-opt}$and the optimal tip-speed ratio λ_{opi} [32].

The active power of the bypass rotor is controlled for maximum wind power. Furthermore, to maintain the magnet level and access the interactive capability setting (i.e. working in the PF unit), the interactive capability must be controlled. Maximum energy consumption is obtained by controlling the required mechanical energy with the generator speed rotation at its optimum rate, according to the concept of power signal feedback based on current mode control. The rotary bypass adapter, as shown in Figure 4, is often used to control the speed of the generator. It allows the generator to adapt the rotational speed based on the best wind energy tracking.

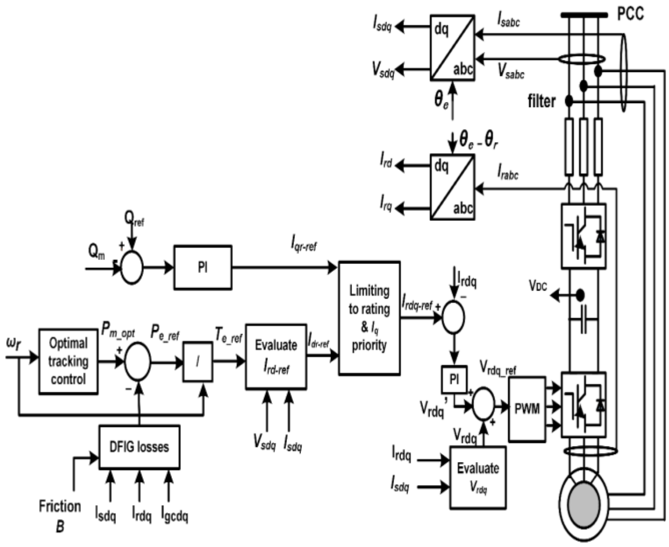

Fig. 4. Control scheme of rotor side converter.

The photovoltaic station consists of many cells connected in series and in parallel to provide the requested output voltage and current. The photovoltaic module is a semiconductor diode made of a p-n junction that turns on the light. In series photovoltaic cells, the resistor (R_s) is connected in series with the parallel coupling with the photo-current source (I_{ph}), the inserted diode (D), and the shunt resistor (R_{sh}). The equivalent circuit of the photovoltaic cell is shown in Fig. 5. When the system is exposed to sunlight, any particle has an energy level greater than the finite gap energy of the spent p-n diode and finds the electron-hole pair corresponding to the radiation. The energy production of photovoltaic panels is affected by the intensity of solar energy, the temperature, and the angle of inclination. This can be summarized as follows [33-37]:

$$E_{pv} = N_{pv} \times P_{rate} \times \eta_{pv} \times \frac{G}{G_{ref}} \times [1 - \beta_t\,(T_c - T_{cref})] \tag{17}$$

$$T_c = T_a + \left(NOCT - \frac{20}{800}\right) G \tag{18}$$

Where T_c is the cell temperature, T_a is the ambient temperature, T_{cref} is the cell temperature under standard conditions, $NOCT$ is the nominal operating cell temperature, N_{pv} is the number of PV modules, G is the site's average global solar irradiation, G_{ref} denotes solar radiation under standard test conditions., η_{pv} is the PV module efficiency.

Each PV module is connected to a DC/DC boost converter to give maximum power while varying the solar radiation. In addition, the PV modules are connected in parallel with the VSI. The importance of VSI lies in maintaining DC link voltage stability, injecting active power into the power grid, and obtaining the required reactive power. The electrical energy supplied by the PV module to the system can be summarized as follows:

$$I = I_{pv} - I_o\left[\exp\left(\frac{V + R_s I}{V_{th}^{a}}\right) - 1\right] - \frac{V + R_s I}{R_p} \tag{19}$$

$$P_{pv} = \eta_{inv}\, I V_{dc} \tag{20}$$

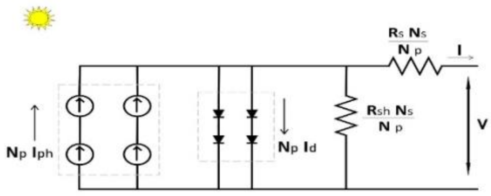

Fig. 5. The PV module equivalent circuit.

Where I is the output current, V is the output voltage, R_s is the series resistance, R_p refers to the shunt resistance, I_{ph} is the photocurrent delivered by the current source, I_o is the saturation current of the diode, V_{th} refers to the thermal voltage, P_{pv} is the output power, η_{inv} is refer to the efficiency of the photovoltaic.

Also, the PSO and PO algorithms are used to calculate the optimal value of K_p and K_i in the PI control circuit (K_p=2.9, K_i=1.2). The system is tested with and without D-FACTS during overloading, switching the capacitor bank and short circuit faults (single line-to-ground, double line-to-ground, and three line-to-ground) separately as shown in Fig.3. In the presence of SVC with short circuit fault, heavy load and nonlinear load connecting to the point of common coupling.

7. Simulation Results

Different scenarios have been demonstrated to validate the effectiveness of the proposal controller such as:

a) The proposed system is examined against the harmonic distortion that occurs by the nonlinear load (universal bridge). The THD level without D-FACTS was unacceptable according to Table 1. Harmonic spectrum shown in Fig. 6. The proposed work after using SVC and D-STATCOM, the THD level has reduced as shown in Fig. 7 and 9 respectively.

b) Also, the studied system is tested during switching a capacitor bank at the PCC with and without D-FACTS as shown in Fig. 10.

c) A very heavy load is suddenly applied at the PCC with and without D-FACTS as shown in Fig. 12.

d) In the last test case, the system was examined during different faults and its voltage level is recorded in Table 2. In this case voltage level is not accepted technically, therefore, the system is reinforced by D-STATCOM and SVC.

After using SVC, the voltage has improved to the accepted value even with overloading condition as shown in Fig 12. But SVC failed to improve the voltage to reach the accepted value during short circuit faults as shown in Fig. 11 and it failed to reduce the THD to the accepted level. After using D-STACOM during short circuit faults, overloading, switching capacitor bank and nonlinear load connecting both separately the voltage has improved to the accepted value at each condition. The voltage sag, voltage swell, and harmonic distortion are reduced after using D-STATCOM, furthermore, DSTATCOM shows efficient voltage recovery compared with SVC as shown in Figs. 10-12. and Table 2.

7.1 The system without D-FACTS

As shown in the first study case, adding a nonlinear load to the system in the PCC increased the harmonic distortion and measured the THD, as shown in the Fig. 6. In the case of the second study, when switching the capacitor bank in the PCC for 0.4 s, the voltage magnitude increased from 1 pu to 1.5 pu. In the third case, different thrust circuit faults are placed at a common coupling point for 0.2 s. In the case of a single line-to-ground fault, the voltage magnitude decreased from 1 pu to 0.83 pu at PCC voltage as shown in Table 2. Additionally, the voltage magnitude decreased to 0.39 pu in the case of the double line-to-ground fault as shown in the Fig. 11. In the three-line-to-ground fault condition, when the fault resistance R_{on} = 0.5 Ω the voltage decreased to 0.55 pu at the PCC voltage as indicated also in Table 2. After adding a heavy load to the system in the fourth case, the voltage decreased to 0.85 pu as shown in Fig. 12.

7.2 The effect of SVC

The parameters of the SVC device, which are used to improve the power system's performance, are found in [38]. After adding the SVC to the studied system at the PCC, SVC could improve the voltage magnitude to the accepted value during a heavy load condition as shown in Fig. 12. Also SVC has enhanced the voltage level from 0.7 to 0.75 pu in double line to ground fault condition as shown in Fig. 11. It can also enhance another short circuits faults voltage as shown in Table 2. SVC has success to reduce the harmonic distortion (THD) from 11.36% to 5.90%.

7.3 The effect of DSTATCOM

The best value of K_P and K_i employed in the D-STATCOM PI controllers was determined using the PSO and PO techniques on a hybrid PV-Wind system. After compensation by using the modified D-STATCOM, the THD has reduced from 11.36% to 3.22% as shown in Fig. 9, this value is considered accepted according to IEEE standard presented in Table 1. In the voltage swell case, D-STATCOM has reduced the PCC voltage magnitude from 1.18 pu to 1.02 pu as shown in Fig 10. Also, the PCC voltages after compensation using the D-SATCOM become balanced and accepted value at different short circuit faults and overloading conditions. In single line to ground fault case using DSTATCOM the voltage sag has been improved to the accepted value as shown in Table 2. Also, the voltage magnitude of the double and three line-to-ground faults at PCC has been improved to 0.99 pu and 0.98 pu after using D-STATCOM as shown in Fig 11. In the last case, adding a sudden heavy load to the system, the D-STATCOM could raise the voltage magnitude from 0.85 pu to 0.99 pu as shown in Fig.12 and Table 2. Comparing D-STATCOM with the other FACTS, D-STATCOM is considered one of the best. It is thought to be the fastest in terms of voltage control. D-STATCOM can maintain full compensation current even at low line voltage. By self-generation or reactive power absorption, it can also control the output power and provide power oscillatory damping.

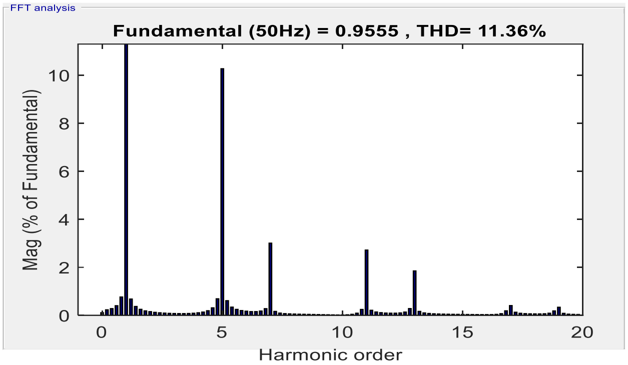

Fig. 6. The THD without FACTS.

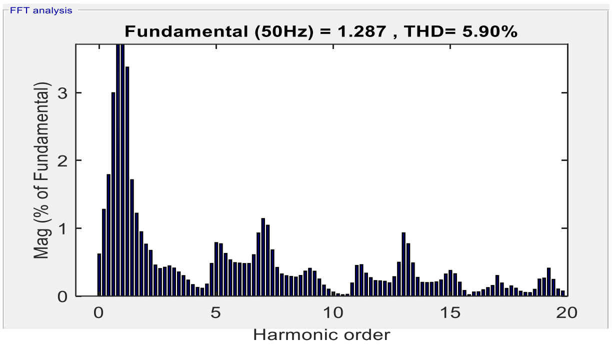

Fig. 7. The THD using SVC.

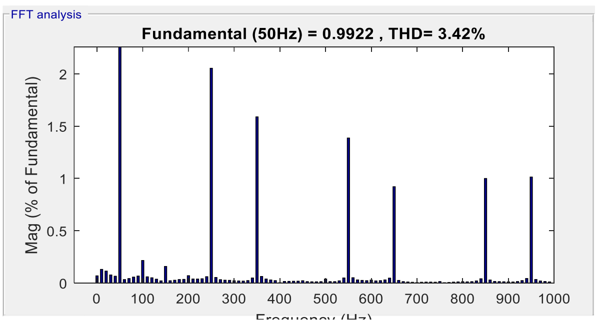

Fig. 8. The THD using D-STATCOM without tuning the paramters.

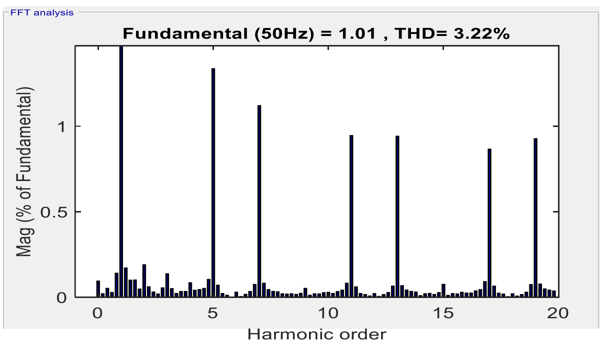

Fig. 9. The THD using D-STATCOM with optimal values of K_p and K_i.

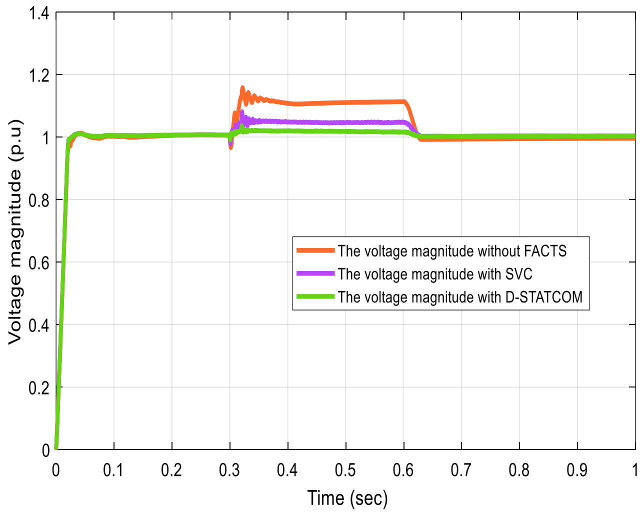

Fig. 10. The voltage magnitude at PCC during capacitor bank switching.

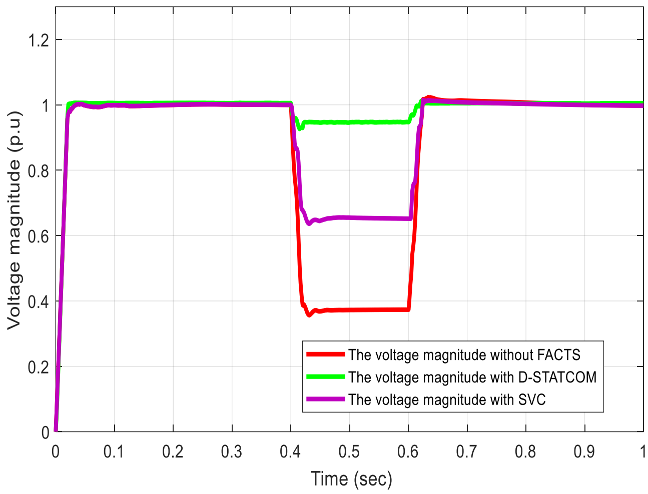

Fig. 11. The voltage magnitude at PCC during double line to ground fault.

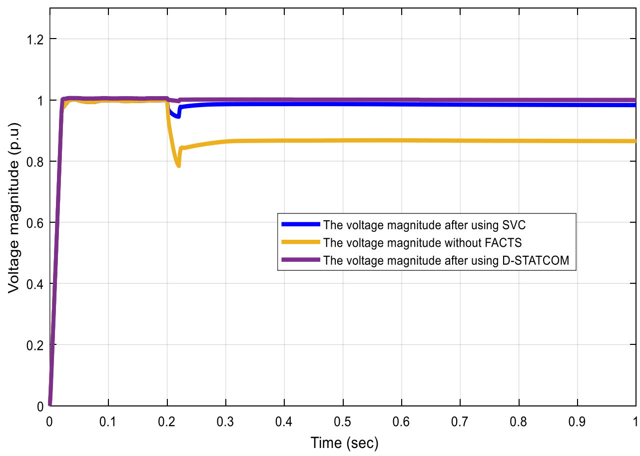

Fig. 12. The voltage magnitude at PCC during overloading with and without FACTS.

Table 2. The voltage magnitude at the PCC during short circuit faults and overloading with and without D-FACTS.

D-FACTS	The voltage magnitude (p.u)			
	SLG	DLG	3-Φ	Overloading
Without FACTS	0.83	0.39	0.55	0.85
SVC	0.88	0.65	0.6	0.98
DSTATCOM without tuning the parameter	0.98	0.98	0.96	0.97
DSTATCOM with Optimal K_p,K_i	0.99	0.99	0.98	0.99

8. Conclusions

In this paper, modeling and simulation of SVC and D-STATCOM connected with a hybrid PV-wind system are presented by using MATLAB/ SIMULINK software. The proposed D-STATCOM is used for harmonic distortion mitigation. The tuning of PI controller of D-STATCOM is proposed by the PSO and PO techniques. furthermore, the D-STATCOM is used for reducing voltage sag caused by a sudden heavy load and short circuit faults (single line to ground, double line to ground, and three phases to ground faults). Also, it is used for reducing the voltage swell caused by a capacitor bank switching. According to the simulation results, the harmonic distortion, the voltage sag, and the voltage swell are mitigated after using DSTATCOM further, DSTATCOM shows efficient voltage recovery compared with SVC. Where with D-STATCOM the THD decreased to 3.2% while it is 5.9 with SVC, and voltage sag and swell have been mitigated effectively.

References

1. M. S. Devi, "Optimized FOPID controller for power quality enhancement between feeders using interline dynamic voltage restorer". Materials Today Proceedings; ScienceDirect, 2020, 2214-7853.
2. M. K. Hammad , M. A. Elhameed, "Voltage Sag Enhancement of Hybrid PV-wind system using DSTATCOM and SVC". The Egyptian International Journal of Engineering Sciences and Technology, 2022. 37, 49–56.
3. T. Zaveri, N. Zaveri, "Comparison of control strategies for DSTATCOM in three-phase, four-wire distribution system for power quality improvement under various source voltage and load conditions". Electrical Power and Energy Systems, 2012. 43, 582–594.
4. M. A. Mahmud, M. J. Hossain, "Nonlinear DSTATCOM controller design for distribution network with distributed generation to enhance voltage stability". Electrical Power and Energy Systems, 2013. 53, 974–979.
5. R. L. Ribeiro, "A Robust Adaptive Control Strategy of Active Power Filters for Power-Factor Correction, Harmonic Compensation, and Balancing of Nonlinear Loads". IEEE Transaction on Power Electronics, 2012. 27-2.
6. R. Jayaraman, "Analysis of sliding mode controller based DSTATCOM for power quality improvement in distribution power system". Materials Today: Proceedings, 2021. 2214-7853.
7. A. Dheepanchakkravarthy, "Performance analysis of FPGA controlled four-leg DSTATCOM for multifarious load compensation in electric distribution system". Engineering Science and Technology, an International Journal, 2018. 692-703.
8. P. M. Almeida, P. G. Barbosa, "Voltage compensation in multi-grounded distribution network with a three-phase five-wire DSTATCOM". Electric Power Systems Research, 2021. 197.
9. K. R. Devabalaji, K. Ravi, "Optimal Placement and Sizing of DSTATCOM Using Harmony Search Algorithm". Energy Procedia, 2015. 759-765.
10. K. Ravi, K. R. Devabalaji, "DSTATCOM allocation in distribution networks considering load variations using bat algorithm". Ain Shams Engineering Journal, 2017. 391-403.
11. T. Yuvaraj, K. Ravi, "Multi-objective simultaneous DG and DSTATCOM allocation in radial distribution networks using cuckoo searching algorithm". Alexandria Engineering Journal, 2018. 2729-2742.
12. C. Kumar, M. K. Mishra, S. Mekhilef, "A new voltage control strategy to improve performance of DSTATCOM in electric grid". CES Transactions on Electrical Machines and Systems, 2020. 295-302.
13. N. Suresh, "Comparison of Control Algorithms of DSTATCOM for Power Quality Improvement". IEEE journal, 2020. 978-1-7281-839.
14. F. Asna, "DSTATCOM for distribution system having high PV penetration". journal, IEEE journal, 2020. 2310-2317.
15. B. Singh, S. R. Arya, "An improved control algorithm of DSTATCOM for power quality improvement". Electrical Power and Energy Systems, 2105. 493–504.
16. D. Amoozegar, "DSTATCOM modelling for voltage stability with fuzzy logic PI current controller". Electrical Power and Energy Systems, 2016. 129–135.
17. S. N. Duarte, P. M. Almeida, L. R. Araujo, P. G. Barbosa, "Control algorithm for DSTATCOM to compensate consumer-generated negative and zero

sequence voltage unbalance". Electrical Power and Energy Systems, 2020. 120-105957.

18. Y. Abdelkad, T. Allaoui, C. Abdelkader, "Power Quality Improvement Based on Five-Level Shunt APF Using Sliding Mode Control Scheme Connected to a Photovoltaic" INTERNATIONAL JOURNAL of SMART GRID, ijSmartGrid, 1-2017.

19. M. M. Elkholy, M. A. El-Hameed, A.A. El-Fergany, "Harmonic analysis of hybrid renewable microgrids comprising optimal design of passive filters and uncertainties". Electric Power Systems Research, 2018. 0378-7796.

20. A. R. Gidd, A. D. Gore, S. B. Jondhale, O. V. Kadekar, M. P. Thkre, "Modelling Analysis and performance of a DSTATCOM for Voltage Sag Mitigation in Distribution Network". International Conference on Trends in Electronics and Informatics, 2019. 366-371.

21. S. N. Deepa, A. P. Rozario, M. Kumar, "Improving Grid Power Quality with FACTS Device on Integration of Wind Energy System". IEEE Journal, 2011. 778-7695.

22. S. Rashmi, V. Yarlagadda, "Voltage sag Mitigation Using static VAR Compensator". International Journal of Engineering Research, 2016. 768-771.

23. R. Jayaraman, S. Tummapudi, R. B. Prakash, T. Muni, "Analysis of sliding mode controller based DSTATCOM for power quality improvement in distribution power system". Materials Today, 2021. 2214-7853.

24. P. Mitra, G. Veayamoorthy, "A DSTATCOM Controller Tuned by Particle Swarm Optimization for an Electric Ship Power System". IEEE Journal, 2008. 806-65409.

25. A. Selvakumar, "A New Particle Swarm Optimization Solution to Nonconvex Economic Dispatch Problems". IEEE Transaction on Power Systems, 2007. 22-2007.
26. L. Zou, "Design of reactive power optimization control for electromechanical system based on fuzzy particle swarm optimization algorithm". Microprocessors and Microsystems, 2021. 82-103865.

27. M. Jaberipour, B. Karimi, "Particle swarm algorithm for solving systems of nonlinear equations". Computers and Mathematics with Applications, 2011. 566–576.

28. A. Mei, M. Zhang, "Power supply system scheduling and clean energy application based on adaptive chaotic particle swarm optimization". Alexandria Engineering Journal, 2022. 2074–2087.
29. Q. Askari, I. Younas, M. Saeed, "Political Optimizer: A novel socio-inspired meta-heuristic for global Optimization". Knowledge-Based Systems, 2020, 0950-7051.

30. A. Kasbi, A. Rahali, "Performance improvement of modern variable-velocity wind turbines technology based on the doubly-fed induction generator (DFIG)". International conference on Aspects of Materials Science and Engineering, 2021. 5426- 5432.

31. H. Benbouhenni, Z. Boudjema, A. Belaidi, "A Direct Power Control of the Doubly Fed Induction Generator Based on the Three-Level NSVPWM Technique" INTERNATIONAL JOURNAL of SMART GRID. 2019. 216-226.
32. A. Kasbi, "Performance improvement of modern variable-velocity wind turbines technology based on the doubly-fed induction generator (DFIG) ". Materials Today: Proceedings, 2021. 5426–5432.
33. S. Pindado, J. Cubas, "Simple mathemathical approach to solar cell/panel behavior based on datasheet information". IEEE journal, 2016. 151-163.
34. M. Lawan, A. Aboushady, K. H. Ahmed, "Photovoltaic MPPT Techniques Comparative Review". International Conference on Renewable Energy Research and Application (ICRERA). 2020. 344-351.

35. A. Seck, M. Thiam*, M. Sarr, M. Wade, "Comparative Study of Photovoltaic Models Using Simulation and Experimental Studies". International Journal of Renewable Energy Research. 2022. 1704-1711.

36. M. Sarr, B. Niang, O. Bâ, L. Thiaw. "Optimization of the Penetration Rate in Photovoltaic Power : Case of the Senegalese Electricity Network". IEEE International Conference on Smart Grid. 2020. 115-121.

37. A. Belkaid, I. COLAK, K. Kayisli. "Improving PV System Performance using High Efficiency Fuzzy Logic Control". IEEE International Conference on Smart Grid. 2020. 152-156.

38. S. Rashmi, "Voltage Sag Mitigation Using Static VAR Compensator". International Journal of Engineering Research, 2016, 768-771.